

Shapiro Delays at the Quadrupole Order for Tests of the No-Hair Theorem Using Pulsars around Spinning Black Holes

Pierre Christian,¹ Dimitrios Psaltis,² and Abraham Loeb¹

¹*Harvard-Smithsonian Center for Astrophysics, 60 Garden Street, Cambridge, MA, USA*

²*University of Arizona, 933 N. Cherry Ave., Tucson, AZ, USA*

(Dated: Month date 2015)

One avenue for testing the no-hair theorem is obtained through timing a pulsar orbiting close to a black hole and fitting for quadrupolar effects on the time-of-arrival of pulses. If deviations from the Kerr quadrupole are measured, then the no-hair theorem is invalidated. To this end, we derive an expression for the light travel time delay for a pulsar orbiting in a black-hole spacetime described by the Butterworth-Ipser metric, which has an arbitrary spin and quadrupole moment. We consider terms up to the quadrupole order in the black-hole metric and derive the time-delay expression in a closed analytic form. This allows for fast computations that are useful in fitting time-of-arrival observations of pulsars orbiting close to astrophysical black holes.

I. INTRODUCTION

The no-hair theorem of general relativity [1] states that the dimensionless quadrupole moment of a non-charged black hole, q , satisfies [2]

$$q \equiv \frac{c^4 Q}{G^2 M^3} = - \left(\frac{cS}{GM^2} \right)^2, \quad (1)$$

where M , S , and Q are the black-hole mass, spin angular momentum, and quadrupole moment, respectively. If the quadrupole moment of a black hole is measured to be in contention to equation (1), one of the following possibilities must occur: either the theory of general relativity needs to be modified, or one of our assumptions regarding black-hole solutions to the Einstein equation is invalid (e.g., the cosmic censorship conjecture or the non-existence of closed timelike curves).

While the quadrupole q has so far eluded measurement for any astrophysical black hole, it may become accessible in the near future with time-of-arrival (TOA) analysis of pulsars [3] orbiting close to the supermassive black hole, Sgr A*, at the center of the Milky Way [4, 5]. The recent discovery of PSR J1745–2900, a magnetar orbiting close to Sgr A* [6], generated further interest towards this possibility. While PSR J1745–2900 is both too unstable for precise time delay measurements [7] and located too far from the black hole for relativistic effects to be significant¹, the cluster of stars around Sgr A* should still harbor a significant number of pulsars [4, 9, 10].

The effect of the quadrupole of a black hole on the orbit of a pulsar around it has been studied in Refs. [3, 5, 10]. However, calculations of higher-order effects on the propagation of light itself and, in particular, on the Shapiro time delays in the pulsar TOAs have been focused on lensing effects [11]. Similar calculations of light time travel delays for solar-system experiments have also been performed based on parametric post-Newtonian (PPN) spacetimes with classical quadrupoles [12–14].

Testing the no-hair theorem of black holes (especially when dealing with near-horizon tests) requires using special spacetimes that do not have any pathologies near the horizon. In order to avoid pathologies, such spacetimes do not have necessarily the same behavior as PPN metrics at the quadrupole or higher order [15]. The biggest drawback in calculating the Shapiro time delay for a spacetime with an arbitrary quadrupole moment is related to the fact that the presence of a Carter-like constant is, in general, not guaranteed. Unlike the case for Petrov-type D spacetimes, such as the Kerr metric, the Hamilton-Jacobi equation is not separable and the null geodesic motion is challenging to solve. However, Ref. [16] showed that the coordinate travel time for a null geodesic obeys a Hamilton-Jacobi like equation of motion that allows for the solution to be written in terms of iterative integrals.

In this paper, we used this iterative approach to obtain an expression describing the time delay of light as it propagates in the vicinity of a black hole, taking into account the black-hole mass, spin, and quadrupole moment. As a proof of principle, we use the Ricci flat metric of Butterworth & Ipser [17], but the approach can be easily generalized to any arbitrary metric with different far-field expansions. For this metric, we obtain an expression that

¹ Astrophysical implications of timing delays of pulsars at large distances from their black holes have been considered in a previous work [8].

is analytical and allows for fast calculations to be performed. In §2, we describe our calculations; in the appendix, we compare our calculations to previous results and, in §3, we provide some concluding remarks.

II. CALCULATIONS

A. The metric and inverse metric to second order

An asymptotically flat metric that is both stationary and axisymmetric can be written up to order $(GM/rc^2)^2$ in the quasi-isotropic coordinates (t, r, θ, ϕ) as [17, 18],

$$g_{tt} = -1 + \frac{2GM}{rc^2} - 2 \left(\frac{GM}{rc^2} \right)^2 + \mathcal{O} \left[\left(\frac{GM}{rc^2} \right)^3 \right], \quad (2)$$

$$g_{rr} = 1 + \frac{2GM}{rc^2} + \left(\frac{3}{2} - 2\beta + 4\beta \cos^2 \theta \right) \left(\frac{GM}{rc^2} \right)^2 + \mathcal{O} \left[\left(\frac{GM}{rc^2} \right)^3 \right], \quad (3)$$

$$g_{\phi\phi} = r^2 \sin^2 \theta + r^2 \sin^2 \theta \frac{2GM}{rc^2} + r^2 \sin^2 \theta \left(\frac{3}{2} + 2\beta \right) \left(\frac{GM}{rc^2} \right)^2 + \mathcal{O} \left[\left(\frac{GM}{rc^2} \right)^3 \right], \quad (4)$$

$$g_{\phi t} = -2 \frac{a_* GM^2}{r^3 c^2} r^2 \sin^2 \theta \left(1 + \frac{GM}{rc^2} \right) + \mathcal{O} \left[\left(\frac{GM}{rc^2} \right)^3 \right], \quad (5)$$

$$g_{\theta\theta} = r^2 g_{rr} \quad (6)$$

where $a_* \equiv cS/(GM^2)$ and, following [18], we have defined

$$\beta \equiv (1/4) + \tilde{B}_0/M^2, \quad (7)$$

where \tilde{B}_0 is a multipole of Ref. [17], as the dimensionless parameter characterizing the black-hole. We will now convert this to Cartesian coordinates, set $G = c = 1$, use geometric units (so that distances and times are measured in units of M), and write the metric order by order. To first order, we get

$$g_{tt}^{(1)} = g_{xx}^{(1)} = g_{yy}^{(1)} = g_{zz}^{(1)} = \frac{2}{\sqrt{x^2 + y^2 + z^2}}, \quad (8)$$

where the contravariant metric to first order

$$g_{(1)}^{\mu\nu} = \eta^{\mu\alpha} \eta^{\nu\beta} g_{\alpha\beta}^{(1)}, \quad (9)$$

gives identical components. Similarly, the second order metric $g_{\mu\nu}^{(2)}$ is

$$g_{tt}^{(2)} = -\frac{2}{(x^2 + y^2 + z^2)}, \quad (10)$$

$$g_{xt}^{(2)} = \frac{2a_* y}{(x^2 + y^2 + z^2)^{3/2}}, \quad (11)$$

$$g_{yt}^{(2)} = -\frac{2a_* x}{(x^2 + y^2 + z^2)^{3/2}}. \quad (12)$$

$$g_{xy}^{(2)} = -\frac{4xy\beta}{(x^2 + y^2 + z^2)^2}, \quad (13)$$

$$g_{xx}^{(2)} = \frac{[x^2(3 - 4\beta) + (y^2 + z^2)(3 + 4\beta)]}{2(x^2 + y^2 + z^2)^2}, \quad (14)$$

$$g_{yy}^{(2)} = \frac{[y^2(3 - 4\beta) + (x^2 + z^2)(3 + 4\beta)]}{2(x^2 + y^2 + z^2)^2}, \quad (15)$$

$$g_{zz}^{(2)} = \frac{[(x^2 + y^2)(3 - 4\beta) + z^2(3 + 4\beta)]}{2(x^2 + y^2 + z^2)^2}. \quad (16)$$

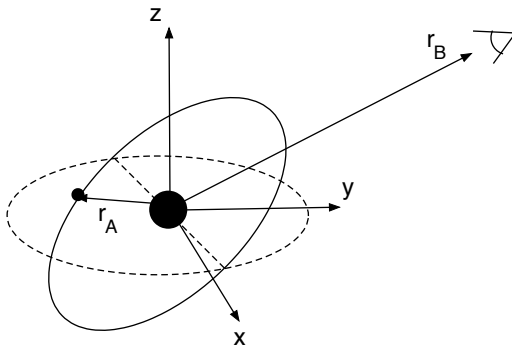


FIG. 1: The geometry used in the calculation. The z -axis of the coordinate system is aligned with the spin of the black hole, the position vector of the pulsar is \mathbf{r}_A , and the position vector of the distant observer is \mathbf{r}_B and lies on the $y - z$ plane.

and the contravariant metric to second order

$$g_{(2)}^{\mu\nu} = \eta^{\mu\alpha}\eta^{\nu\beta}g_{\alpha\beta}^{(2)} + \eta^{\mu\alpha}g_{\alpha\beta}^{(1)}g^{\beta\nu}_{(1)}, \quad (17)$$

becomes

$$g_{(2)}^{tt} = -\frac{6}{(x^2 + y^2 + z^2)}, \quad (18)$$

$$g_{(2)}^{xt} = -\frac{2a_*y}{(x^2 + y^2 + z^2)^{3/2}}, \quad (19)$$

$$g_{(2)}^{yt} = \frac{2a_*x}{(x^2 + y^2 + z^2)^{3/2}}, \quad (20)$$

$$g_{(2)}^{xy} = -\frac{4xy\beta}{(x^2 + y^2 + z^2)^2}, \quad (21)$$

$$g_{(2)}^{xx} = \frac{[x^2(11 - 4\beta) + (y^2 + z^2)(11 + 4\beta)]}{2(x^2 + y^2 + z^2)^2}, \quad (22)$$

$$g_{(2)}^{yy} = \frac{[y^2(11 - 4\beta) + (x^2 + z^2)(11 + 4\beta)]}{2(x^2 + y^2 + z^2)^2}, \quad (23)$$

$$g_{(2)}^{zz} = \frac{[(x^2 + y^2)(11 - 4\beta) + z^2(11 + 4\beta)]}{2(x^2 + y^2 + z^2)^2}. \quad (24)$$

The geodesic equation involves terms, via the Christoffel symbols, that are of second order in the metric and its derivatives. As such, the equation for the null geodesics to second order will, in principle, involve terms that are proportional to M and M^2 (describing the effects of mass), to a_* and a_*^2 (describing frame dragging), to β (describing the effects of the quadrupole), and cross terms proportional to a_*M .

B. Parametrization of the pulsar orbit

In this paper, we concentrate on the effect of the black-hole metric on the light propagation and treat the pulsar orbit parametrically. Relativistic effects on the orbit, calculated in Refs. [3, 5], can be added to our calculation to lowest order by adding time dependences on the orbital parameters. To focus on the effects of the time delays along geodesics, we also neglect phenomena that arise from the velocity of the pulsar.

In the following, we will set a Cartesian coordinate systems centered on the black hole, with the z -axis parallel to the black-hole angular momentum vector (see Figure 1). We also set the y -axis such that the line connecting the black hole and the observer lies on the $y - z$ plane (even though we write our expression in a general vector notation that allows for an arbitrary orientation of the observer). We focus our discussion on the light propagation delay from the pulsar at position \mathbf{r}_A to the observer at \mathbf{r}_B .

For a pulsar in an eccentric orbit with semi-major axis a and eccentricity e , the magnitude of the distance between the pulsar and black hole at an orbital phase corresponding to a true anomaly ν is given by

$$r_A = \frac{a(1 - e^2)}{1 + e \cos \nu}, \quad (25)$$

while the direction of the vector \mathbf{r}_A is given by

$$\hat{n}_A \equiv \frac{\mathbf{r}_A}{r_A} = \mathbf{R}_z(\Omega)\mathbf{R}_y(i)\mathbf{R}_z(\nu)\mathbf{R}_z(\omega)\mathbf{R}_y(-i) \cdot \begin{pmatrix} 0 \\ 1 \\ 0 \end{pmatrix}, \quad (26)$$

where we have made use of the following definitions for the rotation matrices

$$\mathbf{R}_y(\theta) \equiv \begin{pmatrix} \cos \theta & 0 & \sin \theta \\ 0 & 1 & 0 \\ -\sin \theta & 0 & \cos \theta \end{pmatrix}, \quad \mathbf{R}_z(\theta) \equiv \begin{pmatrix} \cos \theta & -\sin \theta & 0 \\ \sin \theta & \cos \theta & 0 \\ 0 & 0 & 1 \end{pmatrix}. \quad (27)$$

In this expression, ω is the argument of periapsis, Ω is the longitude of the ascending node, and i is the inclination of the orbit with respect to the black hole spin.

Our expressions will depend on the angle between \mathbf{r}_A and \mathbf{r}_B , which we will leave expressed as the dot product $\mathbf{n}_A \cdot \mathbf{n}_B$, where $\mathbf{n}_B \equiv \mathbf{r}_B/r_B$. For most of the numerical examples shown in the figures, we will set, for simplicity, the observer along the y axis, such that

$$\mathbf{n}_A \cdot \mathbf{n}_B = \hat{y} \cdot \hat{n}_A = (0 \ 1 \ 0) \cdot \hat{n}_A. \quad (28)$$

We further define the geometric distance between \mathbf{r}_A and \mathbf{r}_B as

$$R_{AB} \equiv \sqrt{r_A^2 + r_B^2 - 2r_A r_B \mathbf{n}_A \cdot \mathbf{n}_B}. \quad (29)$$

C. The first order Shapiro delay

Because arbitrary stationary, axisymmetric spacetimes do not generally admit a fourth constant of motion, solving analytically the null geodesic equation of motion is difficult. However, it was recently observed by Ref. [16] that the coordinate time travelled by light rays obeys Hamilton-Jacobi like equations that allows the light propagation time delay to be written in terms of iterative integrals. In particular, the propagation time delay to first order is given by [16]

$$\Delta^{(1)}(\mathbf{r}_A, \mathbf{r}_B) = \frac{1}{2} R_{AB} \int_0^1 \left[g_{(1)}^{00} - 2N_{AB}^i g_{(1)}^{0i} + N_{AB}^i N_{AB}^j g_{(1)}^{ij} \right]_{\mathbf{z}_+(\mu)} d\mu, \quad (30)$$

where $N_{AB}^i = (r_B^i - r_A^i)/R_{AB}$ and $\mathbf{z}_+(\mu) = \mathbf{r}_A + \mu(\mathbf{r}_B - \mathbf{r}_A)$.

Looking at the contravariant metric to first order, we can identify the first and last term as the well known Shapiro delay effect for non-rotating bodies (up to order 1). This is given by [16]

$$\begin{aligned} \Delta^{(1)}(\mathbf{r}_A, \mathbf{r}_B) &\equiv \int_0^1 \left[g_{(1)}^{00} + N_{AB}^i N_{AB}^j g_{(1)}^{ij} \right]_{\mathbf{z}_+(\mu)} d\mu \\ &= 2 \log \left(\frac{r_A + r_B + R_{AB}}{r_A + r_B - R_{AB}} \right), \end{aligned} \quad (31)$$

where r_A and r_B are the magnitudes of \mathbf{r}_A and \mathbf{r}_B respectively.

In this section, we will express the magnitudes of the various effects on the Shapiro delays in terms of their dependences on the Euclidian distance of closest approach to the light ray from the black hole

$$r_c = \frac{r_A r_B}{R_{AB}} |\mathbf{n}_A \times \mathbf{n}_B|. \quad (32)$$

We, therefore, rewrite equation (31) as

$$\Delta^{(1)}(\mathbf{r}_A, \mathbf{r}_B) \approx 2 \log \left(\frac{r_c + r_A \mathbf{n}_A \times \mathbf{n}_B}{r_c - r_A \mathbf{n}_A \times \mathbf{n}_B} \right), \quad (33)$$

where we used the approximation that for astronomical applications, $r_A \ll r_B$. This shows explicitly the known fact that the magnitude of the first order Shapiro delay is logarithmic in r_c .

D. The second order time delay

The second order contribution to the light time travel delay is given by [16]

$$\begin{aligned} \Delta^{(2)}(\mathbf{r}_A, \mathbf{r}_B) = & \frac{1}{2} R_{AB} \int_0^1 \left\{ \left[g_{(2)}^{00} - 2N_{AB}^i g_{(2)}^{0i} + N_{AB}^i N_{AB}^j g_{(2)}^{ij} \right]_{\mathbf{z}_+(\mu)} \right. \\ & \left. + 2 \left[N_{AB}^j g_{(1)}^{ij} \right]_{\mathbf{z}_+(\mu)} \frac{\partial \Delta^{(1)}}{\partial x^i}(\mathbf{x}_A, \mathbf{z}_+(\mu)) + \eta^{ij} \left[\frac{\partial \Delta^{(1)}}{\partial x^i} \frac{\partial \Delta^{(1)}}{\partial x^j} \right]_{(\mathbf{x}_A, \mathbf{z}_+(\mu))} \right\} d\mu. \end{aligned} \quad (34)$$

This includes terms that are of second order in the mass and spin of the black hole, as well as terms that are of first order in the quadrupole. As such, it describes the second order corrections to the Shapiro time delays, the increase in the light paths because of gravitational lensing, as well as the cross terms between these effects. In this section we obtain analytical forms for this second order time delay for spinning black holes with arbitrary quadrupoles.

1. Mass contribution

We will first consider the second order mass terms in equation (34). These are the terms in the second line of equation (34) together with the $g_{(2)}^{00}$ term in the first line, which have been evaluated in Ref.[16], i.e.,

$$\begin{aligned} \Delta_{\text{mass}}^{(2)} = & \frac{1}{2} R_{AB} \int_0^1 \left\{ g_{(2)}^{00} + N_{AB}^i N_{AB}^j g_{(2),M}^{ij} + 2 \left[N_{AB}^j g_{(1)}^{ij} \right]_{\mathbf{z}_+(\mu)} \frac{\partial \Delta^{(1)}}{\partial x^i}(\mathbf{x}_A, \mathbf{z}_+(\mu)) + \eta^{ij} \left[\frac{\partial \Delta^{(1)}}{\partial x^i} \frac{\partial \Delta^{(1)}}{\partial x^j} \right]_{(\mathbf{x}_A, \mathbf{z}_+(\mu))} \right\} d\mu \\ = & \frac{1}{2} R_{AB} \left[\frac{15 \arccos(\mathbf{n}_A \cdot \mathbf{n}_B)}{2r_A r_B \sqrt{1 - (\mathbf{n}_A \cdot \mathbf{n}_B)^2}} - \frac{8}{r_A r_B (1 + \mathbf{n}_A \cdot \mathbf{n}_B)} \right]. \end{aligned} \quad (35)$$

Here, $g_{(2),M}^{ij}$ refers to the mass contribution to the spatial metric, i.e., the terms that are not proportional to the quadrupole parameter β . Equation (35) takes into account the effect of gravitational lensing on the Shapiro delay. Writing this second order mass contribution as

$$\Delta_{\text{mass}}^{(2)} = \frac{|\mathbf{n}_A \times \mathbf{n}_B|}{r_c} \left[\frac{15 \arccos(\mathbf{n}_A \cdot \mathbf{n}_B)}{4\sqrt{1 - (\mathbf{n}_A \cdot \mathbf{n}_B)^2}} - \frac{4}{(1 + \mathbf{n}_A \cdot \mathbf{n}_B)} \right], \quad (36)$$

we find that this effect is of order $1/r_c$.

2. Spin contribution

The spin contribution to the second order light propagation delay is given by

$$\Delta_{\text{spin}}^{(2)}(\mathbf{r}_A, \mathbf{r}_B) = \frac{1}{2} R_{AB} \int_0^1 \left[-2N_{AB}^i g_{(2)}^{0i} \right]_{\mathbf{z}_+(\mu)} d\mu \quad (37)$$

$$= - \int_0^1 \left[(x_B - x_A) \frac{2a_* y}{(x^2 + y^2 + z^2)^{3/2}} - (y_B - y_A) \frac{2a_* x}{(x^2 + y^2 + z^2)^{3/2}} \right] d\mu. \quad (38)$$

Replacing y and x with $y = y_A + \mu(y_B - y_A)$ and $x = x_A + \mu(x_B - x_A)$, we obtain

$$\Delta_{\text{spin}}^{(2)}(\mathbf{r}_A, \mathbf{r}_B) = - \int_0^1 a_* \left[\frac{-2x_B y_A + 2x_A y_B}{(x^2 + y^2 + z^2)^{3/2}} \right] d\mu. \quad (39)$$

In order to perform this integral, we follow the integration scheme of Ref.[13] with a small modification. We rotate the coordinate axis to the plane defined by \mathbf{r}_A and \mathbf{r}_B .

$$|\mathbf{z}_+(\mu)| = \sqrt{(x^2 + y^2 + z^2)} = \frac{r_c}{\cos(\gamma - \gamma_c)}, \quad (40)$$

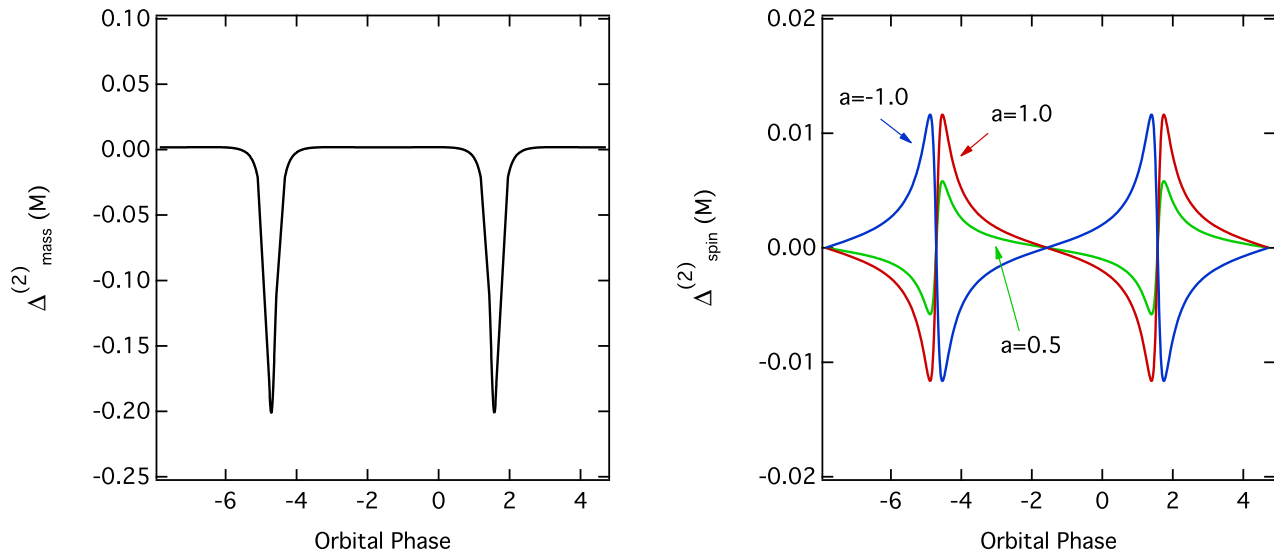


FIG. 2: The second-order contribution due to (*Left*) lensing and (*Right*) frame dragging to the light travel time delay for a pulsar in a circular orbit around a spinning black hole, as a function of orbital phase. The green and red lines in the right panel correspond to black-hole spins of $a = 0.5$ and $a = 1$, respectively, whereas the blue line corresponds to a black hole spinning at $a = 1$ but in the opposite sense with respect to the pulsar orbit. In both panels, the pulsar orbital radius is $1000M$ and its inclination is 80 degrees; the observer is set on the equatorial plane of the black hole; superior conjunction occurs at an orbital phase of $\pi/2$.

where γ is the angle between \mathbf{r}_A and \mathbf{r}_B (defined to be 0 at \mathbf{r}_B) and γ_c is the angle to the point of closest approach. With these expressions and noting that the differential can be expressed as

$$d\mu = \frac{|\mathbf{z}_+(\mu)|^2}{r_c R_{AB}} d\gamma, \quad (41)$$

the integral becomes

$$\int_0^1 \frac{d\mu}{(x^2 + y^2 + z^2)^{3/2}} = \int_0^1 \frac{d\mu}{|\mathbf{z}_+|^3} = \int_{\gamma_A}^{\gamma_B} \frac{\cos(\gamma - \gamma_c)}{r_c^2 R_{AB}} d\gamma = \frac{r_A + r_B}{r_c^2 R_{AB}^2} (1 - \mathbf{n}_A \cdot \mathbf{n}_B). \quad (42)$$

Incorporating this to equation (39), we obtain the second order spin correction to the propagation time delay,

$$\Delta_{\text{spin}}^{(2)}(\mathbf{r}_A, \mathbf{r}_B) = 2a_* (x_B y_A - x_A y_B) \left[\frac{r_A + r_B}{r_A^2 r_B^2} \frac{(1 - \mathbf{n}_A \cdot \mathbf{n}_B)}{|\mathbf{n}_A \times \mathbf{n}_B|^2} \right]. \quad (43)$$

We can obtain the magnitude of the effect described by this equation by noting that

$$(x_B y_A - x_A y_B) = r_A r_B [\mathbf{n}_B - (\mathbf{n}_B \cdot \hat{\mathbf{z}})\hat{\mathbf{z}}] \times [\mathbf{n}_A - (\mathbf{n}_A \cdot \hat{\mathbf{z}})\hat{\mathbf{z}}], \quad (44)$$

allowing us to rewrite equation (43) as

$$\Delta_{\text{spin}}^{(2)}(\mathbf{r}_A, \mathbf{r}_B) \approx \frac{2a_*}{r_c} \frac{[\mathbf{n}_B - (\mathbf{n}_B \cdot \hat{\mathbf{z}})\hat{\mathbf{z}}] \times [\mathbf{n}_A - (\mathbf{n}_A \cdot \hat{\mathbf{z}})\hat{\mathbf{z}}] (1 - \mathbf{n}_A \cdot \mathbf{n}_B)}{\mathbf{n}_A \times \mathbf{n}_B}. \quad (45)$$

This demonstrates that the second-order effect on the Shapiro delay that is due to frame dragging is of order a_*/r_c .

The right panel of Figure 2 shows the second-order contribution to the light time travel delay due to frame dragging for a pulsar in a circular orbit around a black hole as a function of orbital phase. We also compare it (left panel) to the second-order contribution due to lensing derived in the previous section. For the purposes of this figure, we set the pulsar orbital radius to $1000M$, its inclination to 80° , and the observer on the equatorial plane of the black hole. We also varied the spin of the black hole from being retrograde to the orbital motion ($a = -1$) to being prograde ($a = 0, 0.4, 1.04$).

As expected, the contribution due to frame dragging changes sign around orbital phases $\nu = \pi/2$, as the photons from the pulsar to the distant observer change from moving with the direction of frame dragging to moving against it. The fact that at these two phases in a circular orbit, the contribution due to frame dragging vanishes while the contribution due to lensing has its maximum value, makes the overall amplitude of the former to be significantly suppressed compared to the amplitude of the latter effect, even though they both have the same scaling with r_c .

3. Quadrupole contribution

The quadrupole terms in equation (34) are the $g_{(2)}^{ij}$ terms that are proportional to the quadrupole parameter, β . In order to evaluate them, we write

$$\begin{aligned} \frac{1}{2}R_{AB} \left[N_{AB}^i N_{AB}^j g_{(2),Q}^{ij} \right]_{\mathbf{z}_+(\mu)} = & \\ & \beta \frac{(x_B - x_A)^2}{R_{AB}} \frac{-x^2 + y^2 + z^2}{(x^2 + y^2 + z^2)^2} + \beta \frac{(y_B - y_A)^2}{R_{AB}} \frac{-y^2 + x^2 + z^2}{(x^2 + y^2 + z^2)^2} \\ & - \beta \frac{(z_B - z_A)^2}{R_{AB}} \frac{-z^2 + x^2 + y^2}{(x^2 + y^2 + z^2)^2} - 8\beta \frac{(x_B - x_A)(y_B - y_A)}{R_{AB}} \frac{xy}{(x^2 + y^2 + z^2)^2}, \end{aligned} \quad (46)$$

where $g_{(2),Q}^{ij}$ refers to the spatial metric components that are proportional to β . After substituting $\mathbf{r} = \mathbf{r}_A + \mu(\mathbf{r}_B - \mathbf{r}_A)$, we perform the same mathematical trick as before, but this time separating the terms proportional to μ^0 , μ , and μ^2 , and writing them in terms of their coefficients, A , B , and C , i.e.,

$$\begin{aligned} \frac{1}{2}R_{AB} \int_0^1 \left[N_{AB}^i N_{AB}^j g_{(2)}^{ij} \right]_{\mathbf{z}_+(\mu)} d\mu & \\ = \int_0^1 \left[\frac{A}{(x^2 + y^2 + z^2)^2} + \mu \frac{B}{(x^2 + y^2 + z^2)^2} + \mu^2 \frac{C}{(x^2 + y^2 + z^2)^2} \right] d\mu, & \end{aligned} \quad (47)$$

where

$$\begin{aligned} A &\equiv 2[-4x_A(x_A - x_B)y_A(y_A - y_B) - (x_A - x_B)^2(x_A^2 - y_A^2 - z_a^2) \\ &\quad + (y_A - y_B)^2(x_A^2 - y_A^2 + z_a^2) - (x_A^2 + y_A^2 - z_a^2)(z_a - z_B)^2]\beta \\ B &\equiv 4\{x_A^4 - 3x_A^3x_B - x_Ax_B(x_B^2 + 3y_A^2 - 4y_Ay_B + y_B^2 - z_a^2 + z_B^2) + x_A^2(3x_B^2 + 2y_A^2 - 3y_Ay_B + y_B^2 - z_a z_B + z_B^2) \\ &\quad + (x_B^2 + y_A^2 - 2y_Ay_B + y_B^2 + z_a^2 - 2z_a z_B + z_B^2)[y_A^2 - y_Ay_B + z_a(-z_a + z_B)]\}\beta \\ C &\equiv 2\{x_A^4 - 4x_A^3x_B + x_B^4 + y_A^4 - 4x_Ax_B[x_B^2 + (y_A - y_B)^2] + 2x_A^2[3x_B^2 + (y_A - y_B)^2] + 2x_B^2(y_A - y_B)^2 \\ &\quad - 4y_A^3y_B + 6y_A^2y_B^2 - 4y_Ay_B^3 + y_B^4 - z_a^4 + 4z_a^3z_B - 6z_a^2z_B^2 + 4z_a z_B^3 - z_B^4\}\beta. \end{aligned} \quad (48)$$

We can, therefore, write the second order contribution in this case as

$$\Delta_{\text{quad}}^{(2)}(\mathbf{r}_A, \mathbf{r}_B) = [I_0 + I_1 + I_2]_0^1, \quad (49)$$

where the indefinite integrals

$$I_0 \equiv \int \frac{A}{r^4} d\mu, \quad (50)$$

$$I_1 \equiv \int \frac{\mu B}{r^4} d\mu, \quad (51)$$

$$I_2 \equiv \int \frac{\mu^2 C}{r^4} d\mu, \quad (52)$$

can be found in Appendix A.

Figure 3 shows the second-order contribution due to the quadrupole to the light travel time delay for a pulsar in a circular orbit around a black hole. We consider black holes with quadrupole moments characterized by $\beta = -0.5, 0.2$, and 0.5 . The orbital distance of the pulsar is $1000M$, its inclination is 80° , and the observer is placed on the equatorial plane of the black hole.

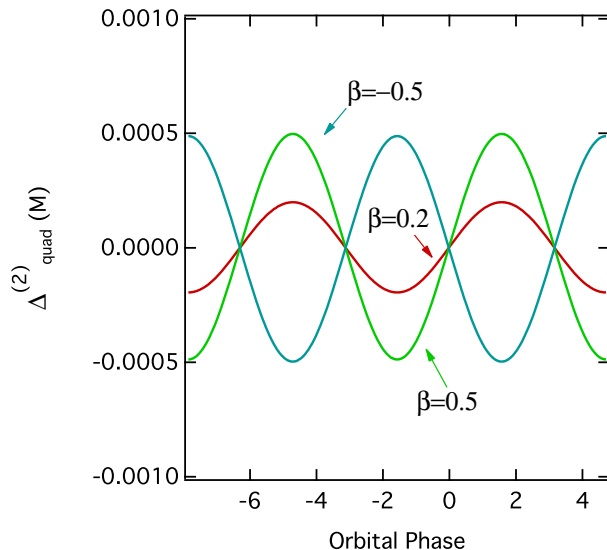


FIG. 3: The second order quadrupole contribution to the light travel time delay for a pulsar in a circular orbit around black holes with different values of the quadrupole parameter β . The orbital radius of the orbit is $1000M$, its inclination is 80° , and the observer is at the equatorial plane of the black hole; superior conjunction occurs at an orbital phase of $\pi/2$.

The overall magnitude of the excursion due to quadrupole is much smaller than lensing and frame-dragging contributions and increases with the magnitude of the black-hole quadrupole. The complicated expressions shown in Appendix A make it hard to obtain the scaling of this effect in an analytical manner. However, as we show in Appendix B, comparing our results with those of Ref. [14], which were obtained using a different approach with harmonic coordinates, allows us to simplify expression (49), for the particular configuration that we are considering here as an example, to

$$\Delta_{\text{quad}}^{(2)} = -\frac{\beta}{2R_{AB}} \left(\frac{r_A^2 - r_B^2 - R_{AB}^2}{r_B^2} + \frac{r_B^2 - r_A^2 - R_{AB}^2}{r_A^2} \right). \quad (53)$$

At the astrophysically relevant limit $r_B \gg r_A$, this expression reduces to

$$\Delta_{\text{quad}}^{(2)} = -\frac{\beta}{r_A} \mathbf{n}_A \cdot \mathbf{n}_B. \quad (54)$$

Comparing this second-order contribution, which scale as the inverse of the orbital distance to the pulsar, to the mass and spin effects derived in the previous subsection, which scale as the inverse of the distance of closest approach of light to the black hole, accounts for the fact that the effect of the quadrupole is significantly smaller for high-inclination observers than those of the mass and the spin.

III. CONCLUSION

In this paper we have provided formulae for the light time travel delays for pulsars orbiting in the spacetime of a black hole, taking into account terms that are up to the quadrupole order. We identified three effects that are, in principle, of the same order. The first effect is expressed in terms that are proportional to the square of the black-hole mass and describe the additional delays due to the lensed trajectories of the photons. The second effect is expressed in terms that are proportional to the black-hole spin and describe the effects of frame dragging. Finally, the last effect describes the influence of the mass quadrupole of the spacetime on the time delays.

We reproduce our expression here for ease of reading, under the astrophysically relevant assumption $r_B \gg r_A$:

$$\begin{aligned}
\Delta^{(1)} &= 2 \log \left(\frac{r_c + r_A \mathbf{n}_A \times \mathbf{n}_B}{r_c - r_A \mathbf{n}_A \times \mathbf{n}_B} \right), \\
\Delta_{\text{mass}}^{(2)} &= \frac{\mathbf{n}_A \times \mathbf{n}_B}{r_c} \left[\frac{15 \arccos(\mathbf{n}_A \cdot \mathbf{n}_B)}{4 \sqrt{1 - (\mathbf{n}_A \cdot \mathbf{n}_B)^2}} - \frac{4}{(1 + \mathbf{n}_A \cdot \mathbf{n}_B)} \right], \\
\Delta_{\text{spin}}^{(2)} &= \frac{2a_*}{r_c} \frac{[\mathbf{n}_B - (\mathbf{n}_B \cdot \hat{z})\hat{z}] \times [\mathbf{n}_A - (\mathbf{n}_A \cdot \hat{z})\hat{z}](1 - \mathbf{n}_A \cdot \mathbf{n}_B)}{\mathbf{n}_A \times \mathbf{n}_B}, \\
\Delta_{\text{quad}}^{(2)} &= [I_0 + I_1 + I_2]_0^1.
\end{aligned} \tag{55}$$

Even though the second-order effects are significantly smaller than the traditional Shapiro delay, their amplitude for the case of a pulsar orbiting a supermassive black hole is not negligible. This is shown in Figure 4, where we plot the amplitude of each effect (defined as the difference between the time delays calculated at the points of superior and inferior conjunction) for different pulsars orbiting the black-hole in the center of the Milky Way, Sgr A*. For reasonable distances of closest approach (see, e.g. discussion in [4, 5, 10]), the amplitudes of these effects are of the order of 100 ms–10 s. These are much larger than the ~ 1 ms measurement uncertainties expected for observations of a pulsar in orbit around Sgr A* with a 100-m dish or the $\lesssim 0.1$ ms uncertainties expected with SKA [5].

At large distances from Sgr A*, the time delay in the pulsar signal may be contaminated by the presence of additional mass between the pulsar and the black hole. The ratio between the leading second-order terms in the metric due to the gravitational field of the black hole and the first-order terms due to the additional enclosed mass scale as [10]

$$\frac{M_{\text{enc}}}{M} \left(\frac{ac^2}{GM} \right) = 4.8 \times 10^{-8} \left(\frac{M_{\text{enc}}}{10^6 M_\odot} \right) \left(\frac{a_0}{1 \text{ pc}} \right)^{-1} \left(\frac{ac^2}{GM} \right)^2, \tag{56}$$

where M_{enc} is the enclosed mass within a distance a_0 from the black hole and we have assumed a radial profile in the density of matter proportional to r^{-2} . In order for the gravitational effects of the enclosed mass to be negligible compared to the second-order effects due to the gravitational field of the black hole, the above ratio has to be smaller than unity, or

$$\frac{ac^2}{GM} \lesssim 4500 \left(\frac{M_{\text{enc}}}{10^6 M_\odot} \right)^{-1} \left(\frac{a_0}{1 \text{ pc}} \right). \tag{57}$$

For pulsars in orbits with larger separations from the black hole, the second order effects we calculated here will not be measurable.

The magnitude of the effects shown in Figure 4 are larger than the orbital effects due to the spacetime quadrupole that were discussed in Ref. [10]. Neglecting the high-order time delay effects, however, will primarily introduce a small bias to the measurement of the quadrupole discussed in Ref. [10] depending on the orientation of the pulsar orbit and observer, since the quadrupole-order time-delay and orbital effects have very different signatures on the pulsar TOAs.

We have also chosen to stop our expansion keeping terms up to the quadrupole order in the black-hole spacetime. Even though this is a reasonable expansion when discussing the metric elements of a slowly spinning black hole, it does not necessarily reflect an appropriate expansion scheme when calculating observables that depend non-linearly on the metric elements. Indeed, Refs. [25] have explored even higher order corrections to the light time travel delays and found that the expansion converges as long as (incorporating back the mass of the black hole) $2Mr_A/r_c^2 \ll 1$. This is an important condition to check when applying our results when the geometric mean of the pulsar orbital radius and the horizon size become comparable to the distance of closest approach of light.

As a final validity check of our analytic expansion, we compared our analytic result to a numerical calculation of light time travel delays using the numerical algorithm of Ref. [26]. In Figure 5 we plot the difference between the light travel time at superior and inferior conjunctions as a function of orbital radius, for a pulsar in circular orbits around a non-spinning black hole at an inclination of 80 degrees. It is clear even from this comparison that second-order effects become important at orbital radii that are of interest to pulsars around the black hole in the center of the Milky Way. Moreover, this comparison demonstrates that our second-order results remain accurate down to distances of closest approach $r_c \sim 60M$ and will, therefore, be useful in the analysis of pulsar observations in this context.

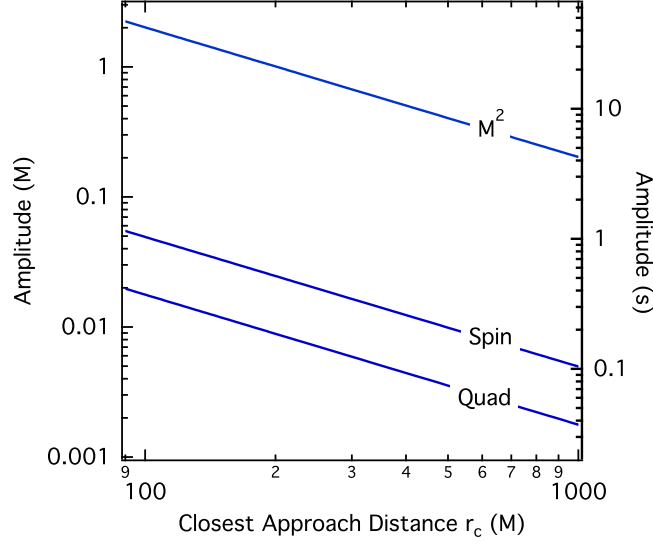


FIG. 4: The amplitudes of the various contributions to the light travel time delay for a pulsar in different circular orbits around a black hole, as a function of the closest approach distance r_c . The inclination of the orbit is 80° , the observer is at the equatorial plane of a Kerr black hole, and the spin of the black hole is maximal. The right axis shows the amplitudes of the various contributions in seconds, for the $4.3 \times 10^6 M_\odot$ mass of Sgr A*. Even though these higher-order effects are small compared to the traditional Shapiro delay, they are much larger than the expected measurement uncertainties for pulsars around Sgr A*.

Appendix A: Expression for the integrals of the quadrupole contribution

The indefinite integrals required to calculate the propagation time delay to second order in equation (52) is given by

$$\begin{aligned}
\int \frac{A}{r^4} d\mu &= (-4x_A(x_A - x_B)y_A(y_A - y_B) - (x_A - x_B)^2(x_A^2 - y_A^2 - z_A^2) \\
&+ (y_A - y_B)^2(x_A^2 - y_A^2 + z_A^2) + (x_A^2 + y_A^2 + z_A^2)(z_A - z_B)^2)\beta((-z_A^2 + z_A z_B + x_A^2(-1 + \mu) + y_A^2(-1 + \mu) + x_B^2\mu + y_B^2\mu + z_A^2\mu \\
&- 2z_A z_B \mu + z_B^2\mu + x_A(x_B - 2x_B\mu) + y_A(y_B - 2y_B\mu)) / ((x_B^2(y_A^2 + z_A^2) + (y_B z_A - y_A z_B)^2 - 2x_A x_B(y_A y_B + z_A z_B) + x_A^2(y_B^2 + z_B^2)) \\
&(z_A^2 + x_A^2(-1 + \mu)^2 + y_A^2(-1 + \mu)^2 - 2z_A^2\mu + 2z_A z_B \mu - 2x_A x_B(-1 + \mu)\mu - 2y_A y_B(-1 + \mu)\mu + x_B^2\mu^2 + y_B^2\mu^2 + z_A^2\mu^2 - 2z_A z_B \mu^2 + z_B^2\mu^2)) \\
&+ ((x_A^2 - 2x_A x_B + x_B^2 + y_A^2 - 2y_A y_B + y_B^2 + z_A^2 - 2z_A z_B + z_B^2)\text{ArcTan} [(-z_A^2 + z_A z_B + x_A^2(-1 + \mu) + y_A^2(-1 + \mu)s \\
&+ x_B^2\mu + y_B^2\mu + z_A^2\mu - 2z_A z_B \mu + z_B^2\mu + x_A(x_B - 2x_B\mu) + y_A(y_B - 2y_B\mu)) / ((x_B^2(y_A^2 + z_A^2) + (y_B z_A - y_A z_B)^2 \\
&- 2x_A x_B(y_A y_B + z_A z_B) + x_A^2(y_B^2 + z_B^2))^{(1/2)}])) / ((x_B^2(y_A^2 + z_A^2) + (y_B z_A - y_A z_B)^2 - 2x_A x_B(y_A y_B + z_A z_B) + x_A^2(y_B^2 + z_B^2))^{3/2}) \\
\int \frac{\mu B}{r^4} d\mu &= 2(2(x_A - x_B)(y_A - y_B)(2x_A y_A - x_B y_A - x_A y_B) - (x_A^2 - x_A x_B + y_A^2 - y_A y_B + z_A(z_A - z_B))(z_A - z_B)^2 \\
&+ (y_A - y_B)^2(-x_A^2 + x_A x_B + y_A^2 - y_A y_B + z_A(-z_A + z_B)) + (x_A - x_B)^2(x_A^2 - x_A x_B - y_A^2 + y_A y_B + z_A(-z_A + z_B))) \\
&\beta((x_A^2(-1 + \mu) + y_A^2(-1 + \mu) - x_A x_B \mu - y_A y_B \mu + z_A(z_A(-1 + \mu) - z_B \mu)) / ((x_B^2(y_A^2 + z_A^2) + (y_B z_A - y_A z_B)^2 \\
&- 2x_A x_B(y_A y_B + z_A z_B) + x_A^2(y_B^2 + z_B^2))(z_A^2 + x_A^2(-1 + \mu)^2 + y_A^2(-1 + \mu)^2 - 2z_A^2\mu + 2z_A z_B \mu - 2x_A x_B(-1 + \mu)\mu - 2y_A y_B(-1 + \mu)\mu \\
&+ x_B^2\mu^2 + y_B^2\mu^2 + z_A^2\mu^2 - 2z_A z_B \mu^2 + z_B^2\mu^2)) + ((x_A^2 - x_A x_B + y_A^2 - y_A y_B + z_A(z_A - z_B)) \\
&\times \text{ArcTan} [(-z_A^2 + z_A z_B + x_A^2(-1 + \mu) + y_A^2(-1 + \mu) + x_B^2\mu + y_B^2\mu + z_A^2\mu - 2z_A z_B \mu + z_B^2\mu \\
&+ x_A(x_B - 2x_B\mu) + y_A(y_B - 2y_B\mu)) / ((x_B^2(y_A^2 + z_A^2) + (y_B z_A - y_A z_B)^2 - 2x_A x_B(y_A y_B + z_A z_B) + x_A^2(y_B^2 + z_B^2))^{(1/2)}])) \\
&/ ((x_B^2(y_A^2 + z_A^2) + (y_B z_A - y_A z_B)^2 - 2x_A x_B(y_A y_B + z_A z_B) + x_A^2(y_B^2 + z_B^2))^{3/2})
\end{aligned}$$

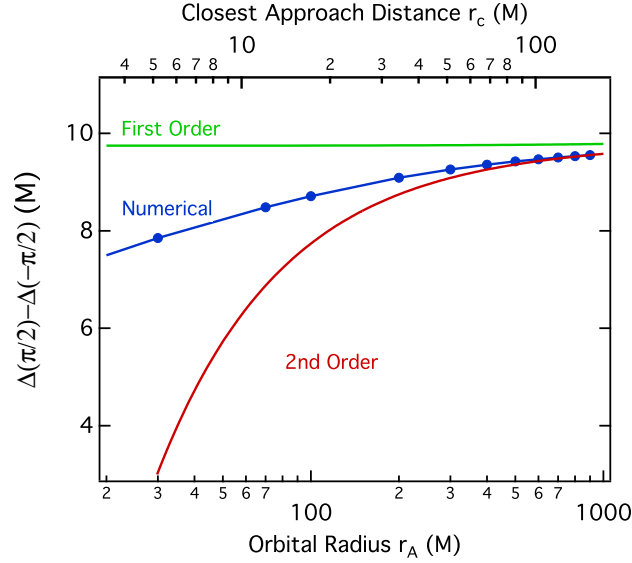


FIG. 5: The difference between the light travel time delay at superior and inferior conjunction as a function of orbital radius for a pulsar in circular orbits around a non-spinning black hole at an inclination of 80° . The green line is the first order Shapiro delay and the red line is our second order calculation. The blue line with the filled circles is the result of a numerical calculation using the algorithm of Ref. [26]. The difference between the numerical result and the first order solution is significant even at large radii. The second order solution becomes inaccurate only at distances of closest approach that are $r_c \lesssim 60$ M.

$$\begin{aligned}
\int \frac{\mu^2 C}{r^4} d\mu = & -2(x_A^4 - 4x_A^3 x_B + x_B^4 + y_A^4 - 4x_A x_B (x_B^2 + (y_A - y_B)^2) + 2x_A^2 (3x_B^2 + (y_A - y_B)^2) \\
& + 2x_B^2 (y_A - y_B)^2 - 4y_A^3 y_B + 6y_A^2 y_B^2 - 4y_A y_B^3 + y_B^4 - z_A^4 + 4z_A^3 z_B - 6z_A^2 z_B^2 + 4z_A z_B^3 - z_B^4) \\
& \beta((-x_A^4 + x_A^3 x_B - 2x_A^2 y_A^2 + x_A x_B y_A^2 - y_A^4 + x_A^2 y_A y_B + y_A^3 y_B - 2x_A^2 z_A^2 \\
& + x_A x_B z_A^2 - 2y_A^2 z_A^2 + y_A y_B z_A^2 - z_A^4 + x_A^2 z_A z_B + y_A^2 z_A z_B + z_A^3 z_B + x_A^4 \mu - 2x_A^3 \\
& x_B \mu + x_A^2 x_B^2 \mu + 2x_A^2 y_A^2 \mu - 2x_A x_B y_A^2 \mu - x_B^2 y_A^2 \mu + y_A^4 \mu - 2x_A^2 y_A y_B \mu + 4x_A x_B y_A y_B \mu - 2y_A^3 y_B \mu - x_A^2 y_B^2 \mu + y_A^2 y_B^2 \mu \\
& + 2x_A^2 z_A^2 \mu - 2x_A x_B z_A^2 \mu - x_B^2 z_A^2 \mu + 2y_A^2 z_A^2 \mu - 2y_A y_B z_A^2 \mu \\
& - y_B^2 z_A^2 \mu + z_A^4 \mu - 2x_A^2 z_A z_B \mu + 4x_A x_B z_A z_B \mu - 2y_A^2 z_A z_B \mu + 4y_A y_B z_A z_B \mu - 2z_A^3 z_B \mu - x_A^2 z_B^2 \mu - y_A^2 z_B^2 \mu + z_A^2 z_B^2 \mu) \\
& / (2(x_A^2 - 2x_A x_B + x_B^2 + y_A^2 - 2y_A y_B + y_B^2 + z_A^2 - 2z_A z_B + z_B^2)) \\
& (x_B^2 y_A^2 - 2x_A x_B y_A y_B + x_A^2 y_B^2 + x_B^2 z_A^2 + y_B^2 z_A^2 - 2x_A x_B z_A z_B - 2y_A y_B z_A z_B + x_A^2 z_B^2 \\
& + y_A^2 z_B^2)(x_A^2 + y_A^2 + z_A^2 - 2x_A^2 \mu + 2x_A x_B \mu - 2y_A^2 \mu + 2y_A y_B \mu - 2z_A^2 \mu + 2z_A z_B \mu + x_A^2 \mu^2 - 2x_A x_B \mu^2 \\
& + x_B^2 \mu^2 + y_A^2 \mu^2 - 2y_A y_B \mu^2 + y_B^2 \mu^2 + z_A^2 \mu^2 - 2z_A z_B \mu^2 + z_B^2 \mu^2)) + ((x_A^2 + y_A^2 + z_A^2) \\
& \text{ArcTan}[(-x_A^2 + x_A x_B - y_A^2 + y_A y_B - z_A^2 + z_A z_B + x_A^2 \mu - 2x_A x_B \mu + x_B^2 \mu + y_A^2 \mu - 2y_A y_B \mu + y_B^2 \mu + z_A^2 \mu - 2z_A z_B \mu + z_B^2 \mu) \\
& / (((x_B^2 y_A^2 - 2x_A x_B y_A y_B + x_A^2 y_B^2 + x_B^2 z_A^2 + y_B^2 z_A^2 - 2x_A x_B z_A z_B - 2y_A y_B z_A z_B + x_A^2 z_B^2 + y_A^2 z_B^2))^{1/2}) \\
& / (2(x_B^2 y_A^2 - 2x_A x_B y_A y_B + x_A^2 y_B^2 + x_B^2 z_A^2 + y_B^2 z_A^2 - 2x_A x_B z_A z_B - 2y_A y_B z_A z_B + x_A^2 z_B^2 + y_A^2 z_B^2)^{3/2}))
\end{aligned}$$

Appendix B: Comparison with other calculations

In this section, we compare the results of our calculations to those of other analytic efforts that employed different approximations and/or methods of solution. We also compare our results to numerical calculations that take into account all multipole moments of a spinning spacetime, in order to explore the range of validity of our approximations.

We do not attempt to compare our results to those of Refs. [11, 23] for two reasons. First, those calculations combine the first-order Shapiro delay terms with the lensing equation, making it hard to identify and compare the

effects of individual orders. Second, the lensing equation gives accurate results when the pulsar is behind the black hole, at a distance that is much larger than the distance of closest approach for light. This approximation is valid only for a very narrow range of orbital phases (very close to $\pi/2$) and observer inclinations (very close to $\pi/2$) and introduces significant errors in more general configurations (see discussion in [24]).

Our results are in detail agreement with the PPN calculations of Ref. [12], who also used a quasi-isotropic coordinate system, when expressed in the appropriate variables.

Ref. [14] calculated the light travel delay for the Schwarzschild metric using the PPN formalism in de Donder (harmonic) coordinates. Their result is

$$\begin{aligned} \Delta_{PPN} = & R_{AB}^D \\ & + 2 \log \left(\frac{r_A^D + r_B^D + R_{AB}^D}{r_A^D + r_B^D - R_{AB}^D} \right) \\ & + 2 \frac{R_{AB}^D}{|\mathbf{r}_B^D \times \mathbf{r}_A^D|} [(r_B^D - r_A^D)^2 - (R_{AB}^D)^2] \\ & + \frac{15}{4} \frac{R_{AB}^D}{|\mathbf{r}_B^D \times \mathbf{r}_A^D|} \cos^{-1}(\mathbf{n}_A \cdot \mathbf{n}_B) \\ & + \frac{1}{8} \frac{1}{R_{AB}^D} \left[\frac{(r_A^D)^2 - (r_B^D)^2 - (R_{AB}^D)^2}{(r_B^D)^2} + \frac{(r_B^D)^2 - (r_A^D)^2 - (R_{AB}^D)^2}{(r_A^D)^2} \right], \end{aligned} \quad (\text{B1})$$

where the superscript D denotes the r-coordinate in the de Donder gauge.

The first term in the above expression corresponds to the geometric delay, while the second term is the first order Shapiro delay. This second term is identical to our first order mass contribution to the time delay given by equation (31), even though they are written in different coordinates. The reason is that the conversion between the r-coordinates of de Donder, r^D , and the radial Schwarzschild coordinate, r_{Sch} , is (where for clarity, we have temporarily reintroduced the black hole mass M into our equations)

$$r^D = r_{\text{Sch}} \left(1 - \frac{M}{r_{\text{Sch}}} \right), \quad (\text{B2})$$

while the conversion between the isotropic radial coordinate (which we use here), r , and the radial Schwarzschild coordinate, r_{Sch} , is

$$r = \frac{r_{\text{Sch}}}{2} \left[1 - \frac{M}{r_{\text{Sch}}} + \left(1 - 2 \frac{M}{r_{\text{Sch}}} \right)^{\frac{1}{2}} \right] \quad (\text{B3})$$

$$\approx r_{\text{Sch}} \left(1 - \frac{M}{r_{\text{Sch}}} \right), \quad (\text{B4})$$

As a result, to first order in M/r , $r \approx r^D$, and our expression is algebraically identical to that of Ref. [14].

To second order in mass, the transformation between r and r^D is given by

$$r \approx r^D - \frac{M^2}{4(r^D)^2}. \quad (\text{B5})$$

It is easily verifiable that plugging this transformations to our equation for the second order mass term in the time delay does not change the algebraic expression, i.e.,

$$\Delta_{\text{mass}}^{(2)} = \frac{R_{AB}^D}{2r_A^D r_B^D} \left[\frac{15 \arccos(\mathbf{n}_A \cdot \mathbf{n}_B)}{2\sqrt{1 - (\mathbf{n}_A \cdot \mathbf{n}_B)^2}} - \frac{8}{(1 + \mathbf{n}_A \cdot \mathbf{n}_B)} \right]. \quad (\text{B6})$$

Using the definition of R_{AB}^D , the third term of the delay in equation (B1) can be manipulated to read

$$2 \frac{R_{AB}^D}{|\mathbf{r}_B^D \times \mathbf{r}_A^D|^2} [(r_B^D - r_A^D)^2 - R_{AB}^D] = - \frac{4R_{AB}^D}{r_A^D r_B^D} \frac{1}{1 + \cos \theta}, \quad (\text{B7})$$

which is the same as the second term of equation (B6). Similarly, a trigonometric identity can be used to transform the fourth term of the delay in equation (B1) into

$$\frac{15}{4} \frac{R_{AB}^D}{|\mathbf{r}_B^D \times \mathbf{r}_A^D|} \cos^{-1}(\mathbf{n}_A \cdot \mathbf{n}_B) = \frac{15R_{AB}^D}{4r_A^D r_B^D} \frac{1}{\sqrt{1 - \cos^2 \theta}}, \quad (\text{B8})$$

which is the same as the first term of equation (B6).

If the orbital configuration of the binary system is such that the $g_{zz}^{(2)}$ term can be ignored, i.e. when the term proportional to $(z_B - z_A)^2$ in equation (46) is small, it is straightforward to identify the last term of equation (B1) with the $\beta = -1/4$ case of equation (49) and write

$$\Delta_{\text{quad}}^{(2)} [I_0 + I_1 + I_2]_{\beta=-1/4} = \frac{1}{8R_{AB}} \left(\frac{r_A^2 - r_B^2 - R_{AB}^2}{r_B^2} + \frac{r_B^2 - r_A^2 - R_{AB}^2}{r_A^2} \right). \quad (\text{B9})$$

We are inspired to seek a similar equivalence for arbitrary β , and by inspection we found that arbitrary quadrupole contributions of (49) in this limit can be written as

$$\Delta_{\text{quad}}^{(2)} = -\frac{\beta}{2R_{AB}} \left(\frac{r_A^2 - r_B^2 - R_{AB}^2}{r_B^2} + \frac{r_B^2 - r_A^2 - R_{AB}^2}{r_A^2} \right). \quad (\text{B10})$$

This serves as a simplification of the complicated equation (49), valid for all orbital configurations in the limit where the $g_{zz}^{(2)}$ term can be ignored. Indeed, for astrophysical purposes where $r_B \gg r_A$, the quadrupole delay in this limit is given by the extremely simple expression

$$\Delta_{\text{quad}}^{(2)}|_{r_B \gg r_A} = -\frac{\beta}{r_A} \mathbf{n}_A \cdot \mathbf{n}_B. \quad (\text{B11})$$

Acknowledgments

We thank Norbert Wex for many useful conversations on Shapiro delays around black holes, for sharing with us M. Ali's Masters thesis, and for pointing us to the appropriate GAIA technical reports. We also acknowledge support from a joint Arizona-Harvard NSF award.

-
- [1] W. Israel, Physical Review, 164, 1776, (1967); W. Israel, Commun. Math. Phys., 8, 245 (1968); B. Carter, Physical Review Letters, 26, 331 (1971); S. W. Hawking, Commun. Math. Phys., 25, 152 (1972); D. C. Robinson, Physical Review Letters, 34, 905 (1975)
 - [2] K. S. Thorne, Reviews of Modern Physics, 52, 299 (1980)
 - [3] N. Wex, & S. M. Kopeikin, ApJ, 514, 388 (1999)
 - [4] E. Pfahl, & A. Loeb 2004, ApJ, 615, 253 (2004); J. M. Cordes et al., NewAR, 48, 1413 (2002)
 - [5] K. Liu et al., ApJ, 747, 1 (2012)
 - [6] J. A. Kennea et al., ApJ, 770, L24 (2013); K. Mori et al., ApJ, 770, L23 (2013); R. P. Eatough, M. Kramer, & B. Klein, et al., in IAU Symposium 291, ed. van Leeuwen, CUP, 291, 382 (2013); R. M. Shannon, & S. Johnston, MNRAS, 435, L29 (2013)
 - [7] V. M. Kaspi et al., astro-ph: 1403.5344 (2014)
 - [8] P. Christian, & A. Loeb, ApJ, 798, 78 (2015)
 - [9] R. S. Wharton, S. Chatterjee, J. M. Cordes et al., ApJ, 753, 108 (2012); J. Chennamangalam, & D. R. Lorimer, MNRAS, 440, L86 (2014); see, however, J. Dexter, & R. M. O'Leary, ApJ, 783, L7 (2014)
 - [10] D. Psaltis, M. Kramer, & N. Wex, ApJ, in press, arXiv:1510.00394 (2015)
 - [11] Lai D., R. Rafikov, ApJ, 621, L41 (2005)
 - [12] G. W. Richter, & R. A. Matzner, Phys. Rev. D , 26, 1219 (1982); G. W. Richter, & R. A. Matzner, Phys. Rev. D , 28, 3007 (1983); G. W. Richter, & R. A. Matzner, Phys. Rev. D , 26, 2549 (1982)
 - [13] P. Teysandier, arxiv/gr-qc/1407.4361 (2014)
 - [14] S. Zschocke, & S. A. Klioner, arXiv: 0904.3704 (2009)
 - [15] see T. Johannsen, Phys. Rev. D , 87, 124017 (2013) and references therein
 - [16] P. Teyssandier, & C. Le Poncin-Lafitte, Classical and Quantum Gravity, 25, 14 (2008)
 - [17] E. M. Butterworth, & J. R. Ipser, ApJ, 200 (1975)
 - [18] M. AlGendy, & S. M. Morsink, ApJ, 791, 78 (2014)
 - [19] R. Blandford, & S. A. Teukolsky, ApJ, 205 (1976)
 - [20] R. Geroch, J. Math. Phys., 11, 2580 (1970)
 - [21] R. O. Hansen, J. Math. Phys., 15, 46 (1974)
 - [22] G. Pappas, & T. A. Apostolatos, Physical Review Letters, 108, 231104 (2012)
 - [23] R. Rafikov, D. Lai, PhysRevD, 73, 6 (2006)
 - [24] M. Ali, Master's Thesis, Bonn University (2011)

- [25] N. Ashby, & B. Bertotti, *Classical and Quantum Gravity*, 27, 145013 (2010); P. Teyssandier, & B. Linet, *Journées 2013 "Systèmes de référence spatio-temporels"*, 24 (2014)
- [26] D. Psaltis, & T. Johannsen, *ApJ*, 745, 1 (2012)